Juno
Magnetometer

Addendum to:

**The Juno Magnetometer (MAG) Standard Product Data
Record and Archive Volume
Software Interface Specification (SIS)**

August 7, 2018
July 18, 2019

DRAFT

Prepared by:

Jack Connerney, Patricia Lawton,
Stavros Kotsiaros & Matija Herceg

Note : This Addendum provides context for and a description of a specific subset of Magnetometer Investigation data files submitted to the Planetary Data System for archive. These files contain data acquired near perijove (only). This material is provided in advance of publication for the purpose of facilitating a data user's understanding of the data formats, processing, and organization. Please treat the contents with confidentiality prior to publication.

1 Introduction

This addendum to the Juno Magnetic Field Investigation Software Interface Specification (SIS) documents data processing, data format, and filename changes that were introduced subsequent to release of the Magnetometer Investigation SIS. These changes only impact data acquired in very strong magnetic fields, and therefore apply only to files spanning perijove passes. For this reason, and for users convenience, we have modified our archive strategy to separate the perijove passes from the rest of the archive, and have introduced an additional file product identified in the filename construct with the perijove number (see Section 4).

All non-pj data files are unchanged in content, format, and filename convention and remain as described in the SIS. These files encompass the entire 53-day orbit during which the instrument remains in the most sensitive dynamic range (range 0). The perijove interval as defined here begins when the outboard instrument ranges up to range 1 (nominally 6400 nT full scale) and continues until the outboard instrument ranges back down to range 0 (nominally 1600 nT dynamic range). The perijove files will typically contain observations within +/- 7 or 8 Rj radial distance of the planet.

2 Reasons for Perijove (PJ) Processing Changes

There are several factors that necessitated a change in Magnetometer (MAG) data processing and related products, some resulting from the changes in the Juno Mission Plan (e.g., remaining in 53-day orbits) and some related to spacecraft magnetic field mitigation. These are discussed in brief here and in more detail in dedicated documents.

2.1 The 53-day Mission Plan

Juno's original Mission Plan accumulated all 32 perijove passes via orbits with a period of 11 days, subsequently (before Jupiter Orbit Insertion, JOI) extended to orbits of 14 days duration. After JOI, with the Juno spacecraft in a 53-day capture orbit, and as a result of concern with regard to operation of the propulsion system, the Project decided to execute the mission remaining in the 53-day orbit. As a result of the mission extension, many perijoves are executed at local times that differ substantially from those originally planned for. This impacted the Magnetometer Investigation because we use co-located star cameras for accurate attitude determination (Connerney et al, 2017) at the sensor. They cannot continuously provide attitude solutions at perijove (when needed most) with Jupiter obscuring the field of view or if overwhelmed by bright objects. So we necessarily reverted to an alternative plan, also discussed in Connerney et al, 2017, whereby we use the spacecraft star cameras (and associated attitude determination apparatus) for continuous attitude solutions, combined with a spacecraft-to-MAG sensor transformation that is periodically determined (with gaps) by direct comparison of the spacecraft attitude solutions with those provided by the MAG Investigations Camera Head Units (CHUs) that are co-located with our magnetic sensors.

2.2 Thermal Distortion of Juno's Solar Array Wing 1

Juno's Magnetometer Boom is an extension of Wing 1, one of Juno's three solar array appendages. Direct comparison of the spacecraft attitude solutions with those provided by the MAG Investigations Camera Head Units revealed a systematic variation in the attitude of the MAG Boom during a perijove pass; the MAG Boom itself proved to be remarkably stable, but as it is affixed to the outer end of the solar array, a distortion of the array perturbs the attitude of the MAG Boom. This was quickly identified as a response of the solar array to the slight increase in temperature of the array due to Jupiter shine: thermal emission from Jupiter. The increase in temperature as indicated by multiple thermal sensors on the array is just a few degrees C (about 5 or 6 degrees, most perijoves) from a baseline temperature of about -130° C, but that is sufficient to alter the Boom (and MAG sensor) attitude by almost 0.1 degrees during a gravity or MWR pass. PeriJove passage at an unusual attitude with thermal implications (e.g., large angle between sc z axis and sun vector, such as PJ19, MWR cross-track) will result in substantially larger thermal distortion. This thermal distortion is brief in duration (few hours) and the array returns to its pre-perijove attitude after thermal relaxation. An attitude determination error of this magnitude would compromise the vector accuracy of the magnetic field measurement (in strong magnetic fields) if not corrected for.

While we did not anticipate significant distortion of the solar array during periJoves due to thermal radiation from Jupiter, perhaps we should have, as the response of the solar array to thermal excursions was well documented in the instrument paper appearing in Space Science Reviews. During cruise, we noted a temperature related attitude variation of about 1 degree in magnitude, largely a rotation about the spacecraft y axis, resulting from the large thermal excursion of the solar array during transit from Earth to Jupiter. This is understood as a result of the different coefficient of thermal expansion of the array materials, carbon-composite face sheeted honeycomb aluminum with solar cells and glass bonded to one face.

2.3 Spacecraft c-kernel Quasi-Periodic Attitude Errors

Another source of spacecraft attitude estimation error was observed for some time and takes the form of a quasi-periodic attitude disturbance (approximately 20 minute period) of about 0.05 degrees amplitude. Root cause was ultimately traced to the thermal distortion of the Stellar Reference Unit (SRU) mounting bracket which is thermally controlled by two heaters operating independently. This error source was only completely understood subsequent to perijove 19, during which an unusual spacecraft attitude was programmed for a brief interval near periapsis (MWR cross-track). This perijove pass was executed with the z axis of the spacecraft oriented 'down' such that the microwave radiometer (MWR) field of view could scan the planet along lines of constant latitude, essentially orthogonal to the usual scan direction, aligned (approximately) with constant longitude. For this exercise, the solar panels were off sun so the maneuver was constrained to a brief interval and the spacecraft Inertial Measurement Unit (IMU) was commanded 'on' during periapsis. The IMU is typically only used for spacecraft attitude maneuvers, and as it consumes significant electrical power, it is 'off' for all other

periapsis passes. We learned that with the IMU on, the quasi-periodic attitude errors vanished; evidently, the spacecraft attitude estimation algorithm largely ignores the SRU input when the IMU is on.

2.4 Spacecraft Magnetic Field Generated by Eddy Currents

Juno is a spinning spacecraft, rotating with a period of ~1 RPM (during much of cruise) or ~2 RPM (at Jupiter) about the symmetry axis of the high gain antenna (close to the spacecraft payload z axis). Like much of the spacecraft mechanical structure, the Magnetometer Boom is fabricated using lightweight aluminum honeycomb panels with carbon composite face sheets. The magnetometer fluxgate sensors are positioned along the centerline of the boom within a small rectangular cutout in the boom – they reside in a hole in the structure. Rotation of the spacecraft in very strong magnetic fields results in the generation of Eddy currents within the conductive structure that act to resist the change in magnetic field that acts on the conductor. While these are weak currents, Eddy currents flowing in close proximity to the MAG sensors contribute to the measured magnetic field at a level (few parts in 10^4) that would also compromise the absolute accuracy of measurement if not corrected for. This effect was recognized as a 2f spin modulation of the magnetic field magnitude that appeared in precisely the same manner throughout all instrument ranges.

We have determined the electrical conductivity of a representative composite panel by laboratory test and confirmed via finite element modeling (COMSOL) that the perturbations we measure are indeed a result of Eddy current generation. The laboratory measurements yielded an electrical conductivity of ~4 x 10^5 S/m for the sample aluminum honeycomb panel, which is about 1% of the electrical conductivity of bulk aluminum. We've developed a method of calculating the spacecraft field that yields results consistent with our COMSOL modeling (described in greater detail by Kotsiaros et al., manuscript in preparation). This allows an easily implemented calculation of the field due to Eddy currents that we then use to correct the measured field. Files of MAG data rendered in spacecraft payload coordinates ("pl") contain both the corrected field measurement (ambient field) and the correction that was applied (field due to Eddy currents). The corrected field is simply the measured field minus that due to Eddy currents.

3 Implementation of Perijove Processing

Perijove processing addresses the issues described above with a set of procedures to model the solar array thermal distortion and encode a time dependent transformation via NAIF c-kernels for each MAG sensor. The spacecraft magnetic field due to Eddy currents is modeled and removed in all instrument dynamic ranges by application of a correction matrix consistent with detailed COMSOL modeling.

3.1 Attitude Determination and Modeling

The magnetometer sensor attitude determination proceeds along the lines of one of the pathways outlined in the Space Science Reviews (SSR) instrument paper, utilizing the spacecraft star cameras for continuous attitude determinations, combined with a transformation from the spacecraft frame to that of the Magnetometer Optical Benches (MOBs). However, in the SSR description, the transformation from spacecraft frame to that of the MOBs was assumed to be a static transformation that might change from one perijove to another but would remain unchanged during each perijove pass. Identification of the thermal distortion of the solar array necessitated implementation of a time dependent transformation between spacecraft and MOB, and that is implemented using the familiar NAIF (Navigation and Ancilliary Information Facility) tools.
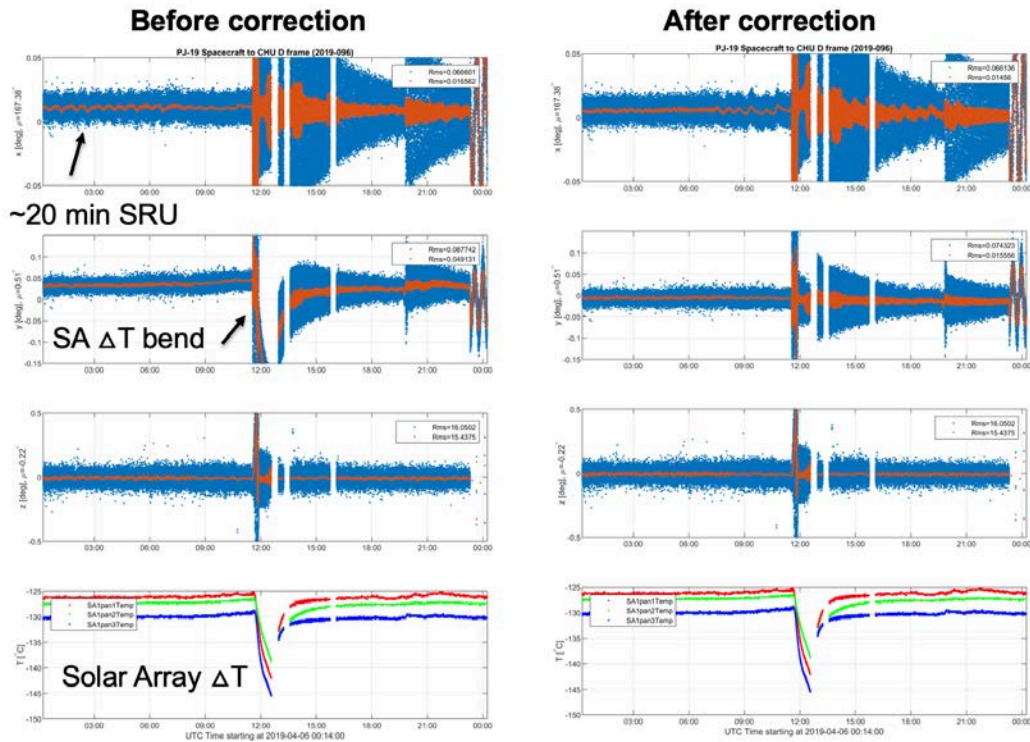

Figure 1: Illustration (from PJ19) of thermal distortion of the solar array. Angular difference between attitude as measured by the MAG ASC (averaged: red curve) and the spacecraft c-kernel through PJ. Top panel is rotation about sc x axis; second panel, y axis;

third panel z axis. Fourth panel is solar array temperature, in this case cooling in response to sc solar arrays going 'off-sun' for the MWR cross-track measurements. On the right, attitude difference after correction using temperature measurements of solar array.

We construct c-kernels for each MOB using a thermo-elastic model of the boom deflection as a function of temperature as fully documented in the accompanying technical note (JUNO-DTU-3114). The model uses temperature measurements from thermistors located on wing 1 to predict the angular deviation experienced during perijove. The angular deviation is almost entirely a rotation about the spacecraft y axis, which is parallel to the solar array hinge line. This behavior is as experienced during cruise from Earth to Jupiter (see Connerney et al., 2017) where ~1 degree of attitude variation (largely about spacecraft y axis) was found in response to the cooling of the array during transit from Earth to Jupiter.
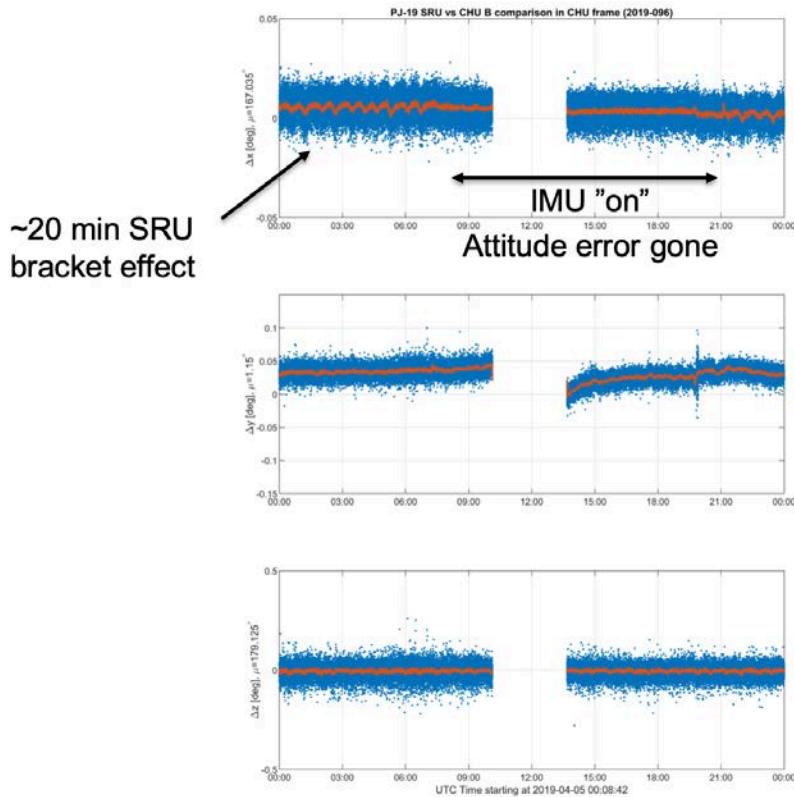

Figure 2: Attitude difference between the MAG ASC attitudes and spacecraft c-kernel for PJ 19, illustrating the disappearance of the quasi-20 minute attitude errors when the sc IMU is 'on'. The quasi-periodic errors in the on-board sc attitude reconstruction result from thermal distortion of the SRU bracket in response to (and correlated with) heater power applied.

The quasi-periodic attitude error introduced into the spacecraft c-kernels by the SRU bracket thermal distortion required a revision of the thermal kernels to correct for this

additional disturbance. Temperature measurements of the SRU bracket (thermistor measurements available in spacecraft engineering) were correlated with the attitude errors (deduced by comparison between SRU quaternions and those produced by the DTU camera head units on the MOB). This allowed for an extension of the model using SRU bracket temperature measurements to (largely, but not completely) correct for the attitude errors. Note, however, that on those rare occasions when the IMU is powered on for a perijove (as in the PJ 19 example illustrated in the figure above) correction for the SRU bracket distortion needs to be turned 'off' if the IMU is on. In figure 1 illustrated above, the distortion is aptly corrected until the IMU comes on, at which point the distortion appears, as it is now 'corrected' when no correction is needed. This will be taken into account in the future (apply correction only when IMU = 'off'). These thermo-elastic MOB c-kernels are provided to NAIF for archive along with the spacecraft c-kernels.

3.2 Eddy Current Modeling and Correction

The vector magnetometer measurements include a small contribution due to Eddy currents circulating in close proximity to the sensor, of a few parts in 10^4 in magnitude, that are most readily apparent, in strong magnetic fields, upon inspection of the magnetic field magnitude. A rotating spacecraft is particularly useful in diagnosing spacecraft-generated magnetic fields that might otherwise go unnoticed on a three axis stabilized platform. This is because a static spacecraft field (or sensor offset) fixed in the spacecraft frame will manifest as a signal in the field magnitude (which ought to be invariant under rotation) at the spin frequency. Conversely a spacecraft-generated field that varies with the applied field magnitude and direction will manifest itself in the field magnitude as a signal at the second harmonic of the spin frequency (as would a scale factor error). Of course, attitude determination errors may also manifest as artifacts at the spin period and multiples thereof. The Eddy current effect is illustrated in Figure 3.
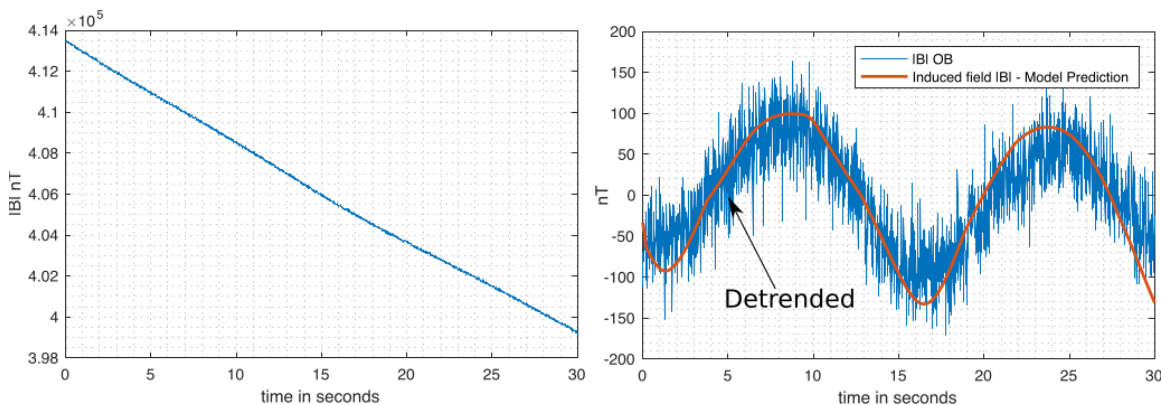

FIGURE 3: Observed field magnitude during one spacecraft rotation in a strong magnetic field (left) and the modulation in (detrended) field magnitude during the rotation arising from Eddy currents generated in the conductive structure near the MAG sensor. The measured field magnitude (blue) evidences rapid excursions due to quantization uncertainty (50 nT quantization step size in the 16 Gauss dynamic range; 16 bit A/D).

Kotsiaros et al. modeled the Eddy current response of the conductive structure in the vicinity of the MAG sensors (manuscript in preparation) to compute the field at the sensor location. The finite element model (COMSOL) uses the physical configuration of the structure around the sensors and a value of the electrical conductivity of the aluminum honeycomb boom panel (6×10^5 S/m) consistent with laboratory measurements (inductive response) on a representative sample of the panel. The gross electrical conductivity of the panel is about 1% of the conductivity of bulk aluminum. Both sensors are positioned in a rectangular cutout straddled by the MOB mounting feet (Figure 4) and thus the conductive structure near each sensor is very similar.
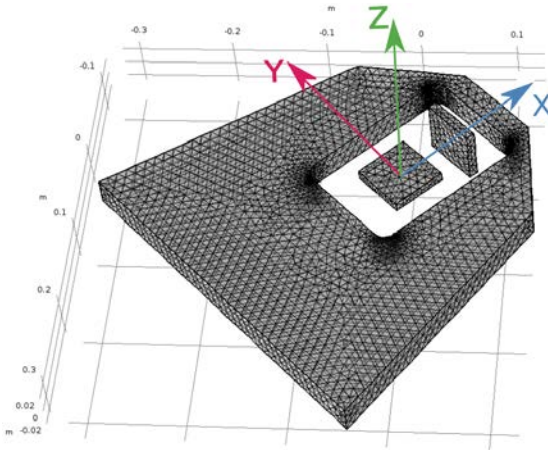

FIGURE 4: Mesh used in finite element modeling of Eddy currents generated in the electrically-conductive aluminum honeycomb panel surrounding the magnetic sensing elements (interior to rectangular cutout). This is a simplified model of the conductive structure near the MAG sensors.

The COMSOL modeling provides guidance regarding the expected amplitude of the field due to Eddy currents and the phase of the response to the applied (sinusoidal) field, in spacecraft payload coordinates. Magnetic field data acquired during perijove, in strong fields, can also be used to characterize the field due to Eddy currents using an analysis similar to the "thin shell" method described in the SSR instrument paper (Connerney et al., 2017). This technique takes advantage of the fact that the field magnitude is invariant under rotation, allows one to find a correction matrix, applied to vector observations, that minimizes variation of the field magnitude under rotation. While only the symmetric part of the correction matrix may be determined by this method, knowledge of the relative magnitude of the variation in payload x and y axes from the COMSOL modeling provides the necessary information to constrain the antisymmetric part. Since the sensor coordinate system is nearly aligned with the spacecraft payload coordinate system, we may correct the measured field in sensor coordinates across all instrument dynamic ranges via application of the following matrix:

```
OB_corrected    = (    0.999800   -0.000286    0.000239   0
                       0.000577    1.000189   -0.000242   0
                      -0.000000   -0.000002    1.000112   0
                       0           0           0          1    )


IB_corrected    = (    0.999792   -0.000299    0.000205   0
                       0.000565    1.000181    0.000258   0
                      -0.000015    0.000000    1.000022   0
                       0           0           0          1    )
```

Note that we treat the vector magnetic field as a four vector to preserve instrument dynamic range across all operations.

Alternatively, one may compute the Eddy current contribution by application of the following matrix to the measured field in sensor coordinates:

```
OB_EMX          = (    0.000200    0.000286   -0.000239   0
                      -0.000577   -0.000189    0.000242   0
                       0.000000    0.000002   -0.000112   0
                       0           0           0          1    )


IB_EMX          = (    0.000208    0.000299   -0.000205   0
                      -0.000565   -0.000181   -0.000258   0
                       0.000015    0.000000   -0.000022   0
                       0           0           0          1    )
```

This second set of matrices constitutes the dynamic spacecraft magnetic field model, allows computation of the spacecraft magnetic field across all instrument dynamic ranges[1]. For all perijove measurements, i.e., measurements obtained within instrument dynamic ranges > 0 (ranges 1,2,4,5,6), we compute the Eddy current correction with OB_EMX and IB_EMX and subtract that from the measured field. Perijove files rendered in spacecraft payload coordinates provide the corrected magnetic field vector per the above as well as the spacecraft magnetic field used to correct the measurement at every time step in payload coordinates (variable name 'OB_BDPL').

---

[1] The magnitude of the field due to Eddy currents is very small, compared to the inducing field, and negligible in range 0 (e.g., ≤ 1 nT). We only apply the correction for data segments near periapsis (ranges ≥ 1). Ranges 2,4,5 are our primary calibration ranges for which application of calibration fields in our facility could be monitored with proton precession (absolute field magnitude) sensors.

Note that the instrument calibration remains unchanged, as measured pre-flight and described in detail in the SSR instrument paper (Connerney et al., 2017). Instrument ranges (0,1,2,4,5,6) were calibrated independently; that nearly identical corrections are required for both sensors and all dynamic ranges[2] demonstrates unambiguously that we correct for a spacecraft-generated magnetic field that scales with the field magnitude, consistent with the COMSOL model of Eddy currents generated by spacecraft rotation in a strong magnetic field (Figure 5).

FIGURE 5: Comparison of the field variation during one rotation of the spacecraft in a strong magnetic field (1.5 Gauss) from finite element modeling (COMSOL) with that resulting from application of the EMX matrix listed above (thin lines). The x components are illustrated in blue, y components in red.

4 Data Quality Assessment

Data quality can be assessed at several points in the data processing chain, as MAG data acquired on a spinning spacecraft provides data assessment opportunity as well as its own challenges. In these examples we look at vector MAG data in sc payload coordinates, eliminating artifacts that may arise owing to sc c-kernel attitude errors that remain after the corrections applied per the discussion above. The data have been corrected for Eddy current contributions. Attitude errors may introduce spin frequency artifacts in data transformed to inertial, or nearly inertial coordinate systems, as well as 2 x spin frequency artifacts (e.g., Auster et al., 2002), so an examination of the data in sc payload coordinates provides insight largely independent of the sc attitude determination. Note also that artifacts at the spacecraft spin period and multiples thereof can also arise when a sinusoidal signal is quantized (with a perfect A/D) because the quantization steps are 'bunched' more densely during the part of the cycle where the field changes most rapidly and less densely as the sinusoid approaches its maximum absolute value.
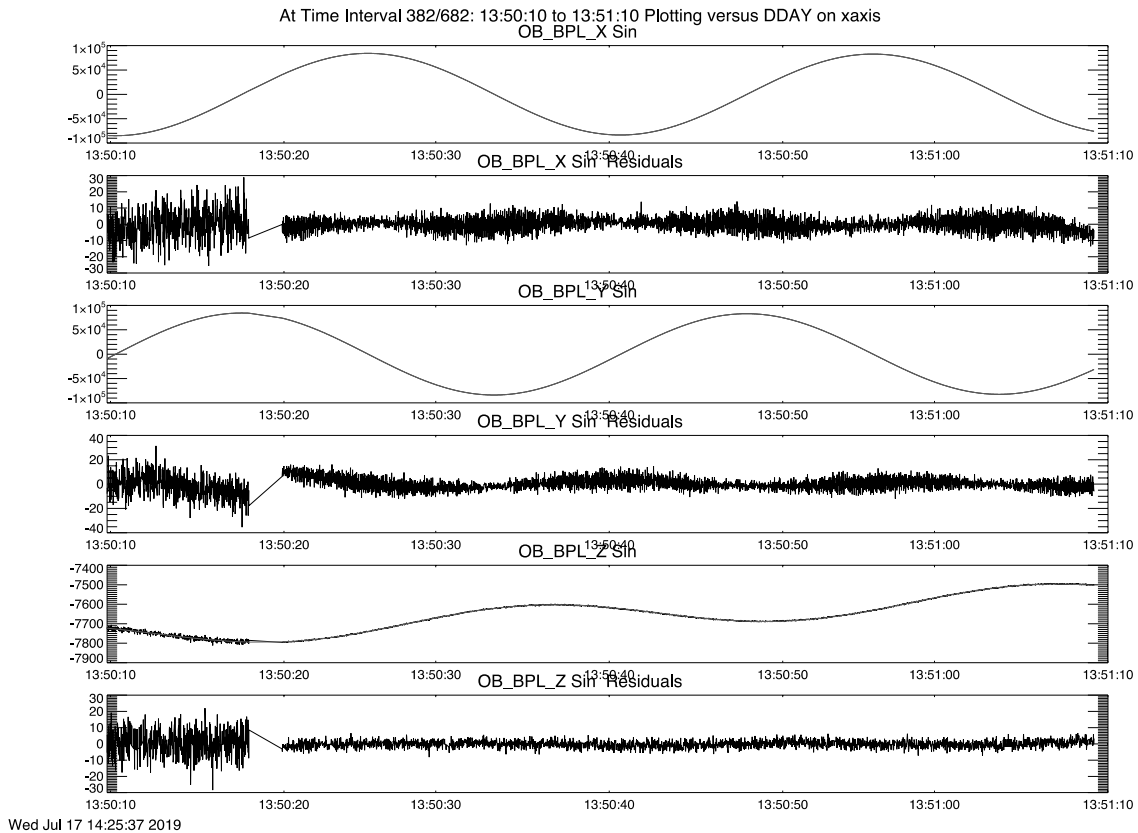

FIGURE 6: Plot of the magnetic field measured by the outboard sensor and difference from a model of vector field variation on a spinning platform. Panels 1, 3, and 5 are the x, y, and z component of the field, and panels 2, 4, and 6 show the difference between the measured field and the model. Sensor transition from instrument range 5 (dynamic range nominally +/- 4.096 Gauss) to sensor dynamic range 4 (nominal dynamic range 1.024 Gauss) occurs near the beginning of the interval just before a 2-second gap during which

the sensor analog response adjusts to the new dynamic range. The plot shows differences consistent with quantization uncertainty, e.g., a few nT in a field of nearly 100,000 nT.

The model applied to each component allows for a constant field, a linear increase in field, and a sinusoidal field with linearly-increasing amplitude. The five parameters are fitted to a few spacecraft spins (allowing for spin period drift, phase) and the model is overplotted on the data (indistinguishable in the figure above) and removed from the measurement (panels 2,4,6) for clarity.

This tool is also useful for examination of field aligned currents which present as deviations in the difference plots; Figure 7 below illustrates one such example. Juno detects Birkeland currents in both weak and very strong field environments.
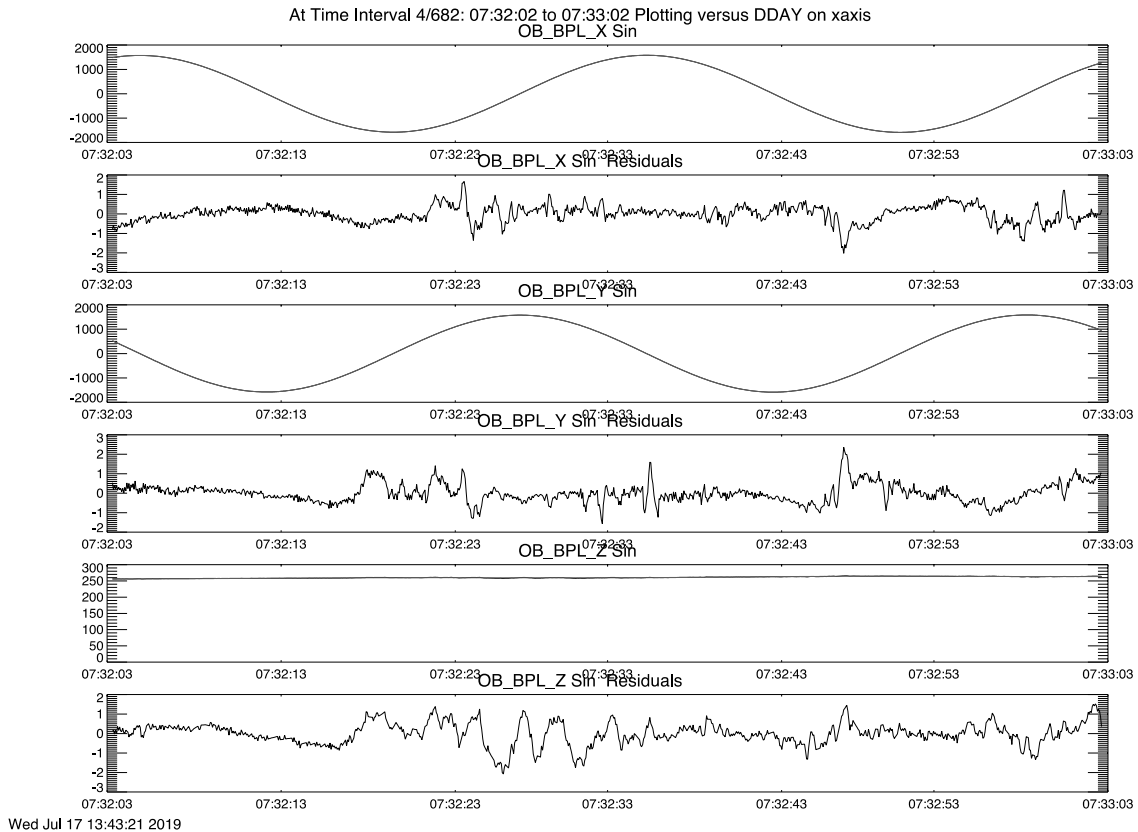

FIGURE 7: Plot of the magnetic field measured by the outboard sensor and difference from a model of vector field variation on a spinning platform. Panels 1, 3, and 5 are the x, y, and z component of the field, and panels 2, 4, and 6 show the difference between the measured field and the model. Differences reveal the presence of field aligned currents that are of relatively small amplitude in the presence of a large background field.

5 File Format and Filename Additions

Perijove data as defined above and processed with the "-sc" option that removes the spacecraft magnetic field are archived in files with filenames that adhere to a slightly different convention. These files are identified via the "_pjPP_' character sequence where 'PP' denotes the perijove number; they are available at multiple sample rates and in multiple coordinate systems as described in the SIS. Like all MAG data products, they contain a self-describing header within which one can identify the command line ("CMD_LINE") that will indicate application of the correction for the spacecraft field via the option "-sc".

Perijove files (e.g., 'fgm_jno_l3_YYYYDDDpc_pjPP_r1s_v01.sts') will be identified via the '_pjPP_' string in the filename, where "PP" denotes the perijove number, and by the year ('YYYY') and day of year ('DDD') of the first day (if two days are required to span a perijove) for which data occurs in the file.

We've added a new variable (OB_BDPL) to the perijove files in payload coordinates to identify the spacecraft magnetic field that was applied to correct the measured field. Addition of this variable expands the data record (payload coordinate files only) by four columns, but attention to the attached ASCII header ought to be sufficient to facilitate reading these files in a transparent manner. The Eddy current correction is provided at every time step along with the corrected magnetic field vector for all payload system files.

5.1 Range Identification in "60 seconds" Resampled Data Files

Juno MAG data is provided in several useful coordinate systems at full time resolution (variable: 64 vectors/s near periJove, elsewhere 32, 16, or 8 samples/s according to telemetry allocation) and also, for convenience, in resampled files with either 1 second or 60 second resolution. These are generated from the high time resolution files using a utility that simply sums each data column over the samples in an interval and divides by the number of samples. As such, the 1-minute resampling may on occasion produce data with range identification equal to 3 (averaging 2 and 4) when the instrument dynamic range changes during an averaging interval.   Range 3 is not a valid instrument range, and should simply be regarded as a 2 to 4 range change flag.

References:

Auster, H. U., K. H. Fornacon, E. Georgescu, K. H. Glassmeier, and U. Motschmann, (2002), Calibration of Fluxgate Magnetometers Using Relative Motion, *Meas. Sci. Technol.* 13, 1124 – 1131.

Connerney, J.E.P., Benn, M., Bjarno, J.B., Denver, T., Espley, J., Jorgensen, J.L., Jorgensen, P.S., Lawton, P., Malinnikova, A., Merayo, J.M., Murphy, S., Odom, J., Oliversen, R., Schnurr, R., Sheppard, D., & Smith, E.J. (2017). The Juno Magnetic Field Investigation, *Space Sci. Rev.,* doi: 10.1007/s11214-017-0334-z.

Herceg, M. and the Juno Magnetometer Team, Micro Advanced Stellar Compass Juno Thermo-elastic stability of Juno wing, Ref: JUNO-DTU-3114, Issue 2.1 Date: July 27, 2018

Kotsiaros, S., Connerney, J. E. P., Martos, Y. M., et al., (2018) Analysis of Eddy Current Generation in the Juno Spacecraft in Jupiter's Magnetic Field, *to be published*.